

# Supplementary Information for “An immersed interface method for the 2D vorticity-velocity Navier-Stokes equations with multiple bodies”

James Gabbard<sup>a</sup>, Thomas Gillis<sup>a</sup>, Philippe Chatelain<sup>b</sup>, Wim M. van Rees<sup>a,\*</sup>

<sup>a</sup>Department of Mechanical Engineering, Massachusetts Institute of Technology, 77 Massachusetts Avenue, Cambridge, MA 02139, USA

<sup>b</sup>Institute of Mechanics, Materials and Civil Engineering, Université Catholique de Louvain, 1348 Louvain-la-Neuve, Belgium

---

---

## S1. Geometry Processing

In the immersed interface method, a solid body is represented entirely by the intersections between a boundary curve and the lines of a Cartesian grid, as well as a normal vector to the boundary at these intersections. Below we present an efficient algorithm which determines these intersections with  $O(h^4)$  accuracy and normal vectors with  $O(h^3)$  accuracy for any object that can be described by a smooth level set.

Let  $\phi(\mathbf{x})$  be a smooth level set satisfying  $\phi(\mathbf{x}) = 0$  on an immersed boundary, and let  $\phi_{ij}$  be its value at the grid point  $\mathbf{x}_{ij}$ . Each control point corresponds to a pair of neighboring points  $\mathbf{x}_{ij}$  and  $\mathbf{x}_{kl}$  for which  $\phi_{ij} < 0$  and  $\phi_{kl} \geq 0$ : because  $\phi(\mathbf{x})$  is continuous, there is a control point  $\mathbf{x}_c$  on the grid-line connecting  $\mathbf{x}_{ij}$  and  $\mathbf{x}_{kl}$  for which  $\phi(\mathbf{x}_c) = 0$ . To locate this intersection efficiently, we limit our attention to the one-dimensional function  $\tilde{\phi}(z) = \phi(\mathbf{x}_{ij} + z(\mathbf{x}_{kl} - \mathbf{x}_{ij}))$ , which restricts  $\phi(\mathbf{x})$  to the grid line connecting  $\mathbf{x}_{ij}$  and  $\mathbf{x}_{kl}$ .

To avoid any additional evaluations of  $\phi$ , we will find the roots of a polynomial which interpolates  $\tilde{\phi}(z)$ . As a first approximation, we find the root of a linear interpolating polynomial, giving  $z_0 = -\phi_{kl}h/(\phi_{kl} - \phi_{ij})$ . This approach locates  $\mathbf{x}_c$  with second order accuracy. To improve on this, we construct a cubic polynomial  $p_3(z)$  which interpolates  $\tilde{\phi}(z)$  at  $z = mh$  for integers  $m$  satisfying  $-1 \leq m \leq 2$ . One root ( $z_1$ ) can be found using Newton’s method with  $z_0$  as an initial guess, and it is likely to lie in  $[0, h]$ . If it does not, we extract a quadratic factor from  $p_3$ , so that

$$\begin{aligned} p_3(z) &= a_3z^3 + a_2z^2 + a_1z + a_0 \\ &= (z - z_1)(b_2z^2 + b_1z + b_0), \quad \text{with} \\ &\begin{cases} b_2 &= a_3, \\ b_1 &= a_2 + z_1b_2, \\ b_0 &= a_1 + z_1b_1. \end{cases} \end{aligned}$$

The remaining two roots of  $p_3$  can then be found with the quadratic formula. One of these roots lies in  $[-h, 0]$ , and provides a fourth order estimate of the location of  $\mathbf{x}_c$ . The normal vector  $\hat{\mathbf{n}} = \nabla\phi(\mathbf{x}_c)/|\nabla\phi(\mathbf{x}_c)|$  can then be calculated with third order accuracy using four-point finite difference stencils and interpolations, as shown in Figure 1.

## S2. Stability of the Transport Discretization

The stability of the free-space transport schemes developed in section 3.1 of the main text can be characterized with a von-Neumann stability analysis, where the velocity field  $\mathbf{u}$  as well as the viscosity  $\nu$  are assumed to be constant in space. For a discretization with grid spacing  $h$  and time step  $\tau$ , stability is dependent on the Fourier number  $r = \nu\tau/h^2$  and the Courant number  $C_{1D} = |u|\tau/h$  for 1D simulations or  $C_{2D} = (|u_x| + |u_y|)\tau/h$  for 2D simulations. Stability regions in the  $(C, r)$  plane for both the 1D and 2D transport schemes with a third order Runge-Kutta time integration scheme are shown in Figure 2. For completeness we also provide the stability regions for a second order Runge-Kutta scheme, although we do not use it in this work.

---

\*Corresponding author. E-mail address: wvanrees@mit.edu

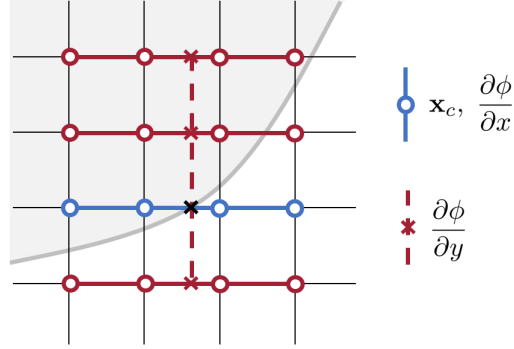


Figure 1: Stencils used to calculate intersection points and normal vectors. The intersection (black cross) is located by fitting a cubic polynomial to the four level set values shown in blue. To calculate the gradient of the level set, the x-direction derivative is taken with the stencil shown in blue, while the y-direction derivative is taken with the stencil shown in red crosses. Each red cross level set value is interpolated using a four point stencil shown in red circles.

Neither the 1D or 2D stability region can be expressed as uncoupled constraints  $0 \leq C \leq C_{max}$  and  $0 \leq r \leq r_{max}$ . Consequently, it is necessary to consider both parameters simultaneously when determining the maximum allowable time step for a given grid resolution. This can be done by noting that the ratio  $C/r = Re_h$  is independent of the time step  $\Delta t$ , so that varying  $\Delta t$  traces out a straight line through the origin of the  $(C, r)$  plane. The maximum allowable time step  $\Delta t_{max}$  corresponds to the intersection between this line and the boundary of the stability region, which can be calculated easily if the boundary is approximated by a series of linear segments. The vertices of a polygon which reasonably approximates each 2D stability region are listed in Table 1.

All of the time-dependent calculations presented in this work use a fixed fraction of the maximum stable time step  $\Delta t = C_{stab}\Delta t_{max}$ , and the constant  $C_{stab}$  is referred to as a “safety factor” in the main text. For the special case of impulsively started flows,  $C_{stab}$  is greatly reduced at the start of each simulation to resolve the initial dynamics, then smoothly brought back to its prescribed value.

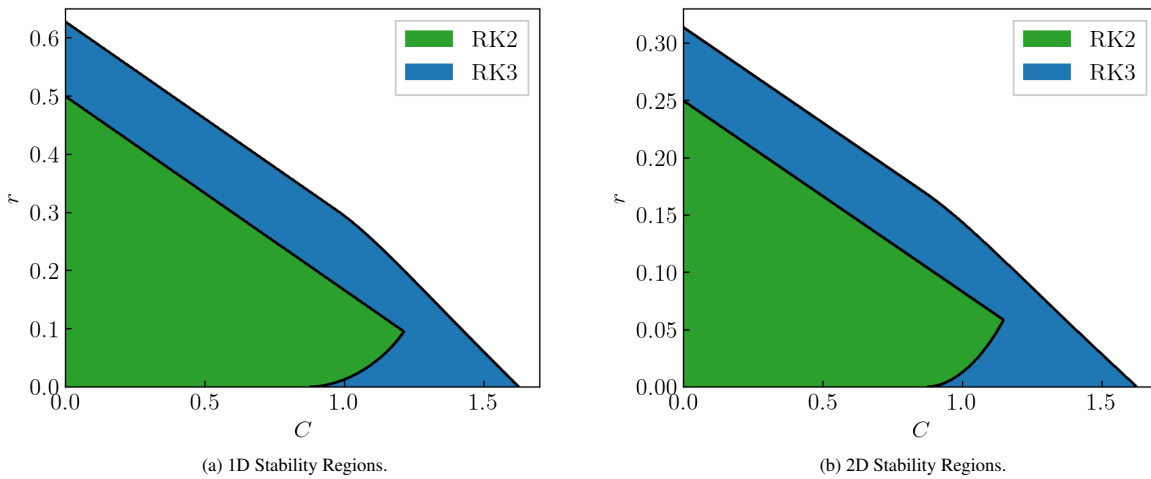


Figure 2: Stability regions for the 1D and 2D transport discretizations with second and third order Runge-Kutta time integration.

### S3. Force Calculation

In a vorticity-based solver, calculating forces and tractions on immersed bodies is complicated by the fact that the pressure field is not immediately available. This section brings together a collection of useful results from across

Time Integration	Vertices ( $C, r$ )
RK3	(0,0), (1.620, 0), (0, 0.314)
RK2	(0,0), (0.874, 0), (1.140, 0.058), (0, 0.250)

Table 1: Stability region of the 2D transport discretization in the ( $C, r$ ) plane, approximated by simple polygons.

the literature which allow 2D vorticity-based methods to circumvent this issue [1, 2, 3]. This includes results which are likely known but difficult to find in print, like (5) and (7), as well as a control volume formulation for calculating moments from only the velocity and vorticity fields (10).

For a stationary body immersed in a two-dimensional flow, the surface traction vector  $\mathbf{t}$  is related to the pressure and the vorticity through

$$\mathbf{t} = -p\hat{\mathbf{n}} + \nu\omega\hat{\mathbf{s}}, \quad (1)$$

where  $\hat{\mathbf{s}} = \hat{\mathbf{k}} \times \hat{\mathbf{n}}$  is the tangential unit vector. Integrating the traction  $\mathbf{t}$  over the surface of a solid body yields the total force vector  $\mathbf{F}$ , while integrating  $(\mathbf{x} - \bar{\mathbf{x}}) \times \mathbf{t}$  yields the total moment  $\mathbf{M}_{\bar{\mathbf{x}}}$  taken about the point  $\bar{\mathbf{x}}$ . These integrals can be broken into two contributions: one from the tangential viscous component  $\mathbf{t}_v = \nu\omega\hat{\mathbf{s}}$ , and one from the normal pressure component  $\mathbf{t}_p = -p\hat{\mathbf{n}}$ . The viscous contribution can be calculated directly from the surface vorticity field, giving

$$\mathbf{F}_v = \nu \oint_S \omega \hat{\mathbf{s}} \, ds, \quad (2)$$

$$\mathbf{M}_{v,\bar{\mathbf{x}}} = \nu \oint_S (\mathbf{x} - \bar{\mathbf{x}}) \times \omega \hat{\mathbf{s}} \, ds. \quad (3)$$

The pressure contribution can be obtained from the Navier-Stokes equations applied to a no-slip boundary,

$$0 = -\nabla p - \nu \nabla \times \omega, \quad (4)$$

which relates the surface pressure gradient directly to the surface vorticity gradient. Using the integral identities

$$\oint_S p \hat{\mathbf{n}} \, ds = - \oint_S \mathbf{x} \times (\hat{\mathbf{n}} \times \nabla p) \, ds, \quad \text{and} \quad \oint_S \mathbf{x} \times p \hat{\mathbf{n}} \, ds = \oint_S \frac{|\mathbf{x}|^2}{2} \hat{\mathbf{n}} \times \nabla p \, ds, \quad (5)$$

the total pressure loads on the body can be written in terms of the normal vorticity gradient:

$$\mathbf{F}_p = \nu \oint_S (\mathbf{x} \times \hat{\mathbf{k}}) \frac{\partial \omega}{\partial n} \, ds, \quad (6)$$

$$\mathbf{M}_{p,\bar{\mathbf{x}}} = \frac{\nu}{2} \oint_S |\mathbf{x} - \bar{\mathbf{x}}|^2 \hat{\mathbf{k}} \frac{\partial \omega}{\partial n} \, ds. \quad (7)$$

Generally, calculations performed on an immersed surface can be significantly noisier than calculations performed on the regular grid. This is compounded by the existence of thin boundary layers in high Reynolds number flows, which lead to large gradients in both velocity and vorticity near no-slip boundaries. Consequently, it is advantageous to have an alternative strategy for calculating the total force and moment on an immersed body that avoids the use of surface quantities. In a vorticity-velocity formulation, this can be done using a control volume approach developed by Noca [1], which does not require explicit knowledge of the the pressure field. Noca’s “momentum 4” formulation, specialized to a stationary immersed obstacle with no-slip boundaries and a stationary 2D control volume, is

$$\mathbf{F} = -\frac{d}{dt} \int_V \mathbf{u} \, dV - \frac{d}{dt} \oint_S \hat{\mathbf{x}} \times (\hat{\mathbf{n}} \times \mathbf{u}) \, dS + \oint_S \hat{\mathbf{n}} \cdot \boldsymbol{\gamma} \, dS. \quad (8)$$

The quantity  $\boldsymbol{\gamma}$  is a tensor collecting miscellaneous terms evaluated on the stationary exterior surface of the control volume,

$$\boldsymbol{\gamma} = \frac{1}{2} |\mathbf{u}|^2 \mathbf{I} - \mathbf{u}\mathbf{u} - \mathbf{u}(\mathbf{x} \times \omega \hat{\mathbf{k}}) + \mathbf{x} \cdot (\nabla \cdot \mathbf{T}) \mathbf{I} - \mathbf{x}(\nabla \cdot \mathbf{T}) + \mathbf{T}, \quad (9)$$

where  $\mathbf{T} = \nu(\nabla \mathbf{u} + \nabla \mathbf{u}^T)$  is the viscous stress tensor. Noca’s work does not include an analogous calculation of the moment acting on an immersed body, but it can be derived using similar methods (see b). Specializing again to an immersed body with no-slip boundaries and a stationary 2D control volume, the analogous expression is

$$\mathbf{M} = -\frac{d}{dt} \int_V \mathbf{x} \times \mathbf{u} \, dV + \frac{d}{dt} \oint_S \frac{|\mathbf{x}|^2}{2} \hat{\mathbf{n}} \times \mathbf{u} \, dS + \oint_S \lambda(\hat{\mathbf{n}}) \, dS. \quad (10)$$

The quantity  $\lambda(\hat{\mathbf{n}})$  collects miscellaneous surface terms, and can be written as the action of a tensor  $\lambda = \mathbf{\Lambda}\hat{\mathbf{n}}$  if necessary (though it is not convenient to do so here):

$$\lambda(\hat{\mathbf{n}}) = \frac{1}{2}|\mathbf{u}|^2(\mathbf{x} \times \hat{\mathbf{n}}) - (\mathbf{x} \times \mathbf{u})(\mathbf{u} \cdot \hat{\mathbf{n}}) - \frac{|\mathbf{x}|^2}{2}\hat{\mathbf{n}} \times (\mathbf{u} \times \omega\hat{\mathbf{k}}) + \frac{|\mathbf{x}|^2}{2}(\nabla \cdot \mathbf{T}) \times \hat{\mathbf{n}} + \mathbf{x} \times (\mathbf{T} \cdot \hat{\mathbf{n}}). \quad (11)$$

These expressions provide the total moment about  $\bar{\mathbf{x}} = 0$ , and can be shifted to any other center by replacing all occurrences of  $\mathbf{x}$  with  $\mathbf{x} - \bar{\mathbf{x}}$ . The surface integrals in this control volume formulation are taken over a rectangular, axis-aligned box that contains the immersed body, and are discretized with the trapezoidal rule. The volume integrals are taken over the regions inside the box, excluding the inside of the immersed obstacle. These are discretized by combining a polynomial extrapolation with the second order level-set integration method developed by Towers [4].

#### S4. Analytical flow field for the impulsively rotated cylinder

The impulsively rotated cylinder with imposed axisymmetry is a flow problem simple enough to have an analytical solution. An expression for the resulting velocity field is provided by Lagerstrom in [5], but little detail on the solution method is provided, and the accompanying expression for the vorticity field is erroneous. Further, the velocity is given in a form which is difficult to evaluate numerically. Here we re-derive Lagerstrom's velocity field and the correct expression for the corresponding vorticity field, then transform both into a form that lends itself to accurate numerical evaluation.

Consider a cylinder of radius  $R$  at rest in an unbounded fluid domain with viscosity  $\nu$ . At  $t = 0$ , the cylinder begins to rotate with angular velocity  $\Omega$ . For convenience we will work in polar coordinates and define the non-dimensional variables  $t^* = \nu t/R^2$ ,  $u^* = u_\theta/\Omega R$ ,  $r^* = r/R$ , and  $\omega^* = \frac{d u^*}{d r^*} = \omega/\Omega$ . In these non-dimensional variables, the Navier-Stokes equations with imposed axisymmetry and a no-slip boundary condition reduce to the one-dimensional linear PDE

$$\begin{aligned} \frac{\partial u}{\partial t} &= \frac{\partial^2 u}{\partial r^2} + \frac{1}{r} \frac{\partial u}{\partial r} - \frac{1}{r^2} u, \\ u(1, t) &= 1, \quad \text{and} \quad \lim_{r \rightarrow \infty} u(r, t) = 0 \\ u(r, 0) &= 0, \end{aligned} \quad (12)$$

where we have dropped the asterisks for readability. This problem can be solved with a Laplace transform for the time variable, which leads to an ODE governing the transformed velocity  $U(r, s)$ :

$$\begin{aligned} r^2 \frac{\partial^2 U}{\partial r^2} + r \frac{\partial U}{\partial r} - (1 + sr^2)U &= 0, \\ U(1, s) &= \frac{1}{s}, \quad \lim_{r \rightarrow \infty} U(r, s) = 0. \end{aligned} \quad (13)$$

The substitution  $\beta = \sqrt{sr}$  transforms this into the modified Bessel equation, which is solved by a linear combination of the two modified Bessel functions,  $U(r, s) = c_1 I_1(\beta) + c_2 K_1(\beta)$ . The arbitrary constants are fixed by applying the boundary conditions, yielding

$$U(r, s) = \frac{1}{s} \frac{K_1(\sqrt{sr})}{K_1(\sqrt{s})}. \quad (14)$$

This is the expression provided by Lagerstrom. Another quantity of interest is the Laplace transform of vorticity field  $W(r, s)$ . Using the definition of vorticity in polar coordinates,

$$W(r, s) = \frac{\partial U}{\partial r} - \frac{U}{r} = -\frac{1}{\sqrt{s}} \frac{K_0(\sqrt{sr})}{K_1(\sqrt{s})}. \quad (15)$$

Applying an inverse Laplace transform, the time-dependent vorticity field is given by

$$\omega(r, t) = -\frac{1}{2\pi i} \int_{\gamma-i\infty}^{\gamma+i\infty} \frac{K_0(\sqrt{sr})}{K_1(\sqrt{s})} \frac{e^{st}}{\sqrt{s}} ds, \quad (16)$$

where  $\gamma$  is an arbitrary positive constant. This integrand oscillates with period  $2\pi/t$  and decays slowly as  $|s| \rightarrow \infty$ , making the integral difficult to approximate by conventional methods. To avoid this we choose to integrate over a

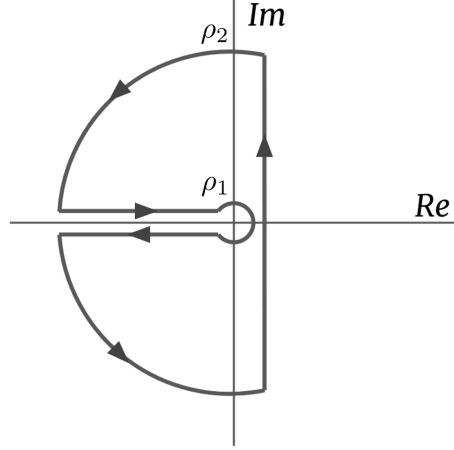


Figure 3: Keyhole contour for the integrand  $W(r, s)e^{st}$  in the complex plane.

different contour in the complex plane. The integrand  $W(r, s)e^{st}$  has a branch cut on the negative real axis (due to the presence of  $\sqrt{s}$  in the expression) and a singularity at  $s = 0$ , but otherwise is analytic. Consequently, the integral of  $W(r, s)e^{st}$  over the closed contour shown in Figure 3 vanishes. We note that the integral along the arcs in the left half-plane vanishes as  $\rho_2 \rightarrow \infty$ , while the integral along the contour encircling the origin vanishes as  $\rho_1 \rightarrow 0$ . Consequently, as the contour grows, the entire integral in (16) is equal and opposite the integrals taken above and below the branch cut:

$$\omega(r, t) = \frac{1}{2\pi i} \int_{-\infty+i\epsilon}^{0+i\epsilon} \frac{K_0(\sqrt{sr})}{K_1(\sqrt{s})} \frac{e^{st}}{\sqrt{s}} ds + \frac{1}{2\pi i} \int_{0-i\epsilon}^{-\infty-i\epsilon} \frac{K_0(\sqrt{sr})}{K_1(\sqrt{s})} \frac{e^{st}}{\sqrt{s}} ds \quad (17)$$

To simplify the integrand further, we make the substitution  $\sqrt{s} = -ix$ , which “unfolds” the path of integration to lie along the real axis. The resulting expression is

$$\omega(r, t) = \frac{1}{\pi} \int_{-\infty}^{\infty} \frac{K_0(ixr)}{K_1(ix)} e^{-x^2 t} dx. \quad (18)$$

This integrand has an even real part and an odd imaginary part, allowing for the simplification

$$\omega(r, t) = \frac{2}{\pi} \int_0^{\infty} \Re \left\{ \frac{K_0(ixr)}{K_1(ix)} \right\} e^{-x^2 t} dx. \quad (19)$$

To avoid complex arithmetic,  $K_\alpha(ix)$  can be re-expressed as a combination of  $J_\alpha(x)$  and  $Y_\alpha(x)$ , the Bessel functions of the first and second kind, giving

$$\omega(r, t) = \frac{2}{\pi} \int_0^{\infty} \frac{J_0(xr)Y_1(x) - J_1(x)Y_0(xr)}{J_1(x)^2 + Y_1(x)^2} e^{-x^2 t} dx. \quad (20)$$

This integrand is non-oscillatory, non-singular at  $x = 0$ , and decays as  $e^{-x^2 t}$  when  $x \rightarrow \infty$ . Consequently, it can be evaluated numerically to any desired degree of accuracy.

The velocity field can be evaluated using the same contour described above, with small alterations. The velocity integrand  $U(r, s)e^{st}$  has a branch cut on the negative real axis and a singularity at  $s = 0$ . However, in this case the singularity is proportional to  $s^{-1}$ , so that the portion of the contour encircling the origin cannot be ignored. Evaluating the additional contribution via residues gives the velocity field

$$u(r, t) = \frac{1}{r} + \frac{2}{\pi} \int_0^{\infty} \Im \left\{ \frac{K_1(ixr)}{K_1(ix)} \right\} \frac{e^{-x^2 t}}{x} dx \quad (21)$$

$$= \frac{1}{r} + \frac{2}{\pi} \int_0^{\infty} \frac{J_1(xr)Y_1(x) - J_1(x)Y_1(xr)}{J_1(x)^2 + Y_1(x)^2} \frac{e^{-x^2 t}}{x} dx. \quad (22)$$

Finally, we evaluate the shear stress and total moment acting on the cylinder's surface. Working now with dimensional variables, the shear stress acting at each point on the cylinder's surface has magnitude  $\tau(t) = \nu\omega(R, t) - 2\nu\Omega$ . The total moment acting on the cylinder is related to the shear stress through  $M(t) = 2\pi R^2\tau(t)$ . Defining a non-dimensional moment  $M^* = M/2\pi R^2\nu\Omega$  then leads to the straightforward non-dimensional relation

$$M^*(t^*) = \omega^*(1, t^*) - 2. \quad (23)$$

### S5. Control volume moment calculation for 3D incompressible flows

There are a variety of methods for using a control volume analysis to obtain the moment acting on an immersed body [6, 7]. It is more difficult, however, to find a formulation that makes no assumptions on the size or position of the control volume, and that does not require the pressure field. In [1], Noca derives a control volume method satisfying these constraints that determines the force on an immersed body. A similar derivation for moments can be done in a completely analogous way; however, it appears to be absent from the literature.

Let  $V(t)$  be a 3D region which contains an immersed solid body. The internal boundary of  $V(t)$  which borders the solid will be denoted  $S_b(t)$ , with a normal vector that points into  $V(t)$  and out of the solid, while the external boundary will be denoted  $S(t)$  with a normal vector that points out of  $V(t)$ . We begin with the conservation of angular momentum for  $V(t)$ ,

$$\begin{aligned} \mathbf{M} = & -\frac{d}{dt} \int_{V(t)} \mathbf{x} \times \mathbf{u} dV + \oint_{S(t)} \mathbf{x} \times [(-p\mathbf{I} + \mathbf{T}) \cdot \hat{\mathbf{n}}] dS \\ & - \oint_{S(t)} (\mathbf{x} \times \mathbf{u})(\mathbf{u} - \mathbf{u}_s) \cdot \hat{\mathbf{n}} dS + \oint_{S_b(t)} (\mathbf{x} \times \mathbf{u})(\mathbf{u} - \mathbf{u}_s) \cdot \hat{\mathbf{n}} dS, \end{aligned} \quad (24)$$

Here  $\mathbf{M}$  is the total moment acting on the immersed body,  $\mathbf{u}_s$  is the velocity of a moving surface,  $\mathbf{I}$  is the identity tensor, and  $\mathbf{T} = \nu(\nabla\mathbf{u} + \nabla\mathbf{u}^T)$  is the viscous stress tensor. To proceed, we use an identity taken from [8],

$$\int_{V(t)} \mathbf{x} \times \mathbf{u} dV = -\frac{1}{2} \int_{V(t)} |\mathbf{x}|^2 \omega dV + \frac{1}{2} \oint_{S(t)} |\mathbf{x}|^2 \hat{\mathbf{n}} \times \mathbf{u} dS - \frac{1}{2} \oint_{S_b(t)} |\mathbf{x}|^2 \hat{\mathbf{n}} \times \mathbf{u} dS. \quad (25)$$

The left hand side represents the total angular momentum of the flow, while the right hand side represents the angular impulse along with boundary terms. Using (25) to replace the first volume integral in (24) gives

$$\begin{aligned} \mathbf{M} = & \frac{d}{dt} \int_{V(t)} \frac{|\mathbf{x}|^2}{2} \omega dV - \frac{d}{dt} \oint_{S(t)} \frac{|\mathbf{x}|^2}{2} \hat{\mathbf{n}} \times \mathbf{u} dS + \frac{d}{dt} \oint_{S_b(t)} \frac{|\mathbf{x}|^2}{2} \hat{\mathbf{n}} \times \mathbf{u} dS \\ & + \oint_{S(t)} \mathbf{x} \times [(-p\mathbf{I} + \mathbf{T}) \cdot \hat{\mathbf{n}}] dS - \oint_{S(t)} (\mathbf{x} \times \mathbf{u})(\mathbf{u} - \mathbf{u}_s) \cdot \hat{\mathbf{n}} dS + \oint_{S_b(t)} (\mathbf{x} \times \mathbf{u})(\mathbf{u} - \mathbf{u}_s) \cdot \hat{\mathbf{n}} dS. \end{aligned} \quad (26)$$

Taking a cue from Noca's derivation, we adopt the following program:

1. Bring the time derivatives inside the integrals over the moving outer surface.
2. Replace all time derivatives of velocity using the Navier Stokes equations.
3. Transform any resulting terms containing  $\nabla p$  into terms containing  $p$  only.

These new pressure terms should exactly cancel the existing pressure term, leaving a pressure-free control volume formulation. To accomplish the first step, we need the tensor identity

$$\frac{d}{dt} \oint_{S(t)} \mathbf{A} \hat{\mathbf{n}} dS = \oint_{S(t)} \frac{\partial \mathbf{A}}{\partial t} \hat{\mathbf{n}} dS + \oint_{S(t)} \nabla \cdot \mathbf{A}(\mathbf{u}_s \cdot \hat{\mathbf{n}}) dS, \quad (27)$$

where  $\mathbf{A}(\mathbf{x}, t)$  is rank-two tensor field and  $(\nabla \cdot \mathbf{A})_i = \sum_j \partial_j A_{ij}$ . Let  $[\mathbf{a}]$  be the cross-product matrix for a vector field  $\mathbf{a}$ , so that  $[\mathbf{a}]\mathbf{x} = \mathbf{a} \times \mathbf{x}$ . Applying (27) to (26) gives

$$\begin{aligned} -\frac{d}{dt} \oint_{S(t)} \frac{|\mathbf{x}|^2}{2} \hat{\mathbf{n}} \times \mathbf{u} dS &= \frac{d}{dt} \oint_{S(t)} \left[ \frac{|\mathbf{x}|^2}{2} \mathbf{u} \right] \hat{\mathbf{n}} dS \\ &= \oint_{S(t)} \frac{\partial}{\partial t} \left[ \frac{|\mathbf{x}|^2}{2} \mathbf{u} \right] \hat{\mathbf{n}} dS + \oint_{S(t)} \nabla \cdot \left[ \frac{|\mathbf{x}|^2}{2} \mathbf{u} \right] (\mathbf{u}_s \cdot \hat{\mathbf{n}}) dS \end{aligned} \quad (28)$$

Noting that  $\nabla \cdot [\mathbf{a}] = -\nabla \times \mathbf{a}$ ,

$$\begin{aligned} &= \oint_{S(t)} \frac{|\mathbf{x}|^2}{2} \frac{\partial \mathbf{u}}{\partial t} \times \hat{\mathbf{n}} \, dS - \oint_{S(t)} \nabla \times \left( \frac{|\mathbf{x}|^2}{2} \mathbf{u} \right) (\mathbf{u}_s \cdot \hat{\mathbf{n}}) \, dS \\ &= - \oint_{S(t)} \frac{|\mathbf{x}|^2}{2} \hat{\mathbf{n}} \times \frac{\partial \mathbf{u}}{\partial t} \, dS - \oint_{S(t)} \left( \mathbf{x} \times \mathbf{u} + \frac{1}{2} |\mathbf{x}|^2 \boldsymbol{\omega} \right) (\mathbf{u}_s \cdot \hat{\mathbf{n}}) \, dS. \end{aligned} \quad (29)$$

In the last step the vector identity  $\mathbf{x} \times \mathbf{a} = -\frac{1}{2} |\mathbf{x}|^2 \nabla \times \mathbf{a} + \frac{1}{2} \nabla \times (|\mathbf{x}|^2 \mathbf{a})$  has been used. To eliminate the time derivative of velocity, we use the Navier Stokes equations in rotational form,

$$\frac{\partial \mathbf{u}}{\partial t} = -\nabla \left( p + \frac{1}{2} |\mathbf{u}|^2 \right) + \mathbf{u} \times \boldsymbol{\omega} + \nabla \cdot \mathbf{T}.$$

Substituting this into the first term of (29),

$$\begin{aligned} - \oint_{S(t)} \frac{|\mathbf{x}|^2}{2} \hat{\mathbf{n}} \times \frac{\partial \mathbf{u}}{\partial t} \, dS &= - \oint_{S(t)} \frac{|\mathbf{x}|^2}{2} \hat{\mathbf{n}} \times \left( -\nabla \left( p + \frac{1}{2} |\mathbf{u}|^2 \right) + \mathbf{u} \times \boldsymbol{\omega} + \nabla \cdot \mathbf{T} \right) \, dS \\ &= \oint_{S(t)} \frac{|\mathbf{x}|^2}{2} \hat{\mathbf{n}} \times \nabla \left( p + \frac{1}{2} |\mathbf{u}|^2 \right) \, dS \\ &\quad - \oint_{S(t)} \frac{|\mathbf{x}|^2}{2} \hat{\mathbf{n}} \times (\mathbf{u} \times \boldsymbol{\omega}) \, dS - \oint_{S(t)} \frac{|\mathbf{x}|^2}{2} \hat{\mathbf{n}} \times (\nabla \cdot \mathbf{T}) \, dS. \end{aligned} \quad (30)$$

The last two integrals on the right hand side do not involve the pressure, and will not be manipulated further. To transform the pressure gradient term in (30), we use the integral identity

$$\oint_{S(t)} \frac{|\mathbf{x}|^2}{2} \hat{\mathbf{n}} \times \nabla \phi \, dS = \oint_{S(t)} \mathbf{x} \times \phi \hat{\mathbf{n}} \, dS. \quad (31)$$

Applying this to the first integral in (30) gives,

$$\begin{aligned} \oint_{S(t)} \frac{|\mathbf{x}|^2}{2} \hat{\mathbf{n}} \times \nabla \left( p + \frac{1}{2} |\mathbf{u}|^2 \right) \, dS &= \oint_{S(t)} \mathbf{x} \times \left( p + \frac{1}{2} |\mathbf{u}|^2 \right) \hat{\mathbf{n}} \, dS \\ &= \oint_{S(t)} \mathbf{x} \times p \hat{\mathbf{n}} \, dS + \oint_{S(t)} \mathbf{x} \times \frac{1}{2} |\mathbf{u}|^2 \hat{\mathbf{n}} \, dS. \end{aligned} \quad (32)$$

To collect these results, we substitute (32) into (30), then substitute (30) into (29), and finally substitute (29) into (26). Canceling the pressure terms and collecting the surface terms brings us to an angular-impulse based control volume formula for moments,

$$\mathbf{M} = \frac{d}{dt} \int_{V(t)} \frac{|\mathbf{x}|^2}{2} \boldsymbol{\omega} \, dV + \frac{d}{dt} \oint_{S_b(t)} \frac{|\mathbf{x}|^2}{2} \hat{\mathbf{n}} \times \mathbf{u} \, dS + \oint_{S_b(t)} (\mathbf{x} \times \mathbf{u})(\mathbf{u} - \mathbf{u}_s) \cdot \hat{\mathbf{n}} \, dS + \oint_{S(t)} \lambda(\hat{\mathbf{n}}) \, dS, \quad (33)$$

where the quantity  $\lambda(\hat{\mathbf{n}})$  collects miscellaneous surface terms:

$$\begin{aligned} \lambda(\hat{\mathbf{n}}) &= \mathbf{x} \times \frac{1}{2} |\mathbf{u}|^2 \hat{\mathbf{n}} - \frac{|\mathbf{x}|^2}{2} \hat{\mathbf{n}} \times (\mathbf{u} \times \boldsymbol{\omega}) - \frac{|\mathbf{x}|^2}{2} \hat{\mathbf{n}} \times (\nabla \cdot \mathbf{T}) - \left( \frac{1}{2} |\mathbf{x}|^2 \boldsymbol{\omega} \right) (\mathbf{u}_s \cdot \hat{\mathbf{n}}) \\ &\quad + \mathbf{x} \times (\mathbf{T} \cdot \hat{\mathbf{n}}) - (\mathbf{x} \times \mathbf{u})(\mathbf{u} \cdot \hat{\mathbf{n}}). \end{aligned} \quad (34)$$

We are now free to use (25) to transform the above back into a formulation based on angular momentum. Doing so removes the integral over the immersed boundary, in exchange for an extra integration around the edge of the domain:

$$\mathbf{M} = -\frac{d}{dt} \int_{V(t)} \mathbf{x} \times \mathbf{u} \, dV + \frac{d}{dt} \oint_{S(t)} \frac{|\mathbf{x}|^2}{2} \hat{\mathbf{n}} \times \mathbf{u} \, dS + \oint_{S_b(t)} (\mathbf{x} \times \mathbf{u})(\mathbf{u} - \mathbf{u}_s) \cdot \hat{\mathbf{n}} \, dS + \oint_{S(t)} \lambda(\hat{\mathbf{n}}) \, dS. \quad (35)$$

This last equation, when specialized to a 2D stationary body, is the control volume moment formulation presented in (10) and (11).

## References

- [1] F. Noca, On the evaluation of time-dependent fluid-dynamic forces on bluff bodies, Ph.D. thesis, California Institute of Technology, 1997.
- [2] L. J. Zhang, J. D. Eldredge, A viscous vortex particle method for deforming bodies with application to biolocomotion, *International journal for numerical methods in fluids* 59 (2009) 1299–1320.
- [3] S. J. Lee, J. H. Lee, J. C. Suh, Computation of pressure fields around a two-dimensional circular cylinder using the vortex-in-cell and penalization methods, *Modelling and Simulation in Engineering* 2014 (2014).
- [4] J. D. Towers, Finite difference methods for approximating heaviside functions, *Journal of Computational Physics* 228 (2009) 3478–3489.
- [5] P. Lagerstrom, *Laminar Flow Theory*, Princeton University press, Princeton, N.J., 1996.
- [6] M. Bergmann, A. Iollo, Modeling and simulation of fish-like swimming, *Journal of Computational Physics* 230 (2011) 329–348.
- [7] N. Nangia, H. Johansen, N. A. Patankar, A. P. S. Bhalla, A moving control volume approach to computing hydrodynamic forces and torques on immersed bodies, *Journal of Computational Physics* 347 (2017) 437–462.
- [8] J. C. Wu, Theory for aerodynamic force and moment in viscous flows, *AIAA Journal* 19 (1981) 432–441.